

Correlation between Spheroid Formation Ability and Reported Invasiveness of HEK-293, HT-29, MDA-MB-231, and HeLa Cancer Cell Lines in Commercial Well Plates

İsmail EŞ¹ 

¹Department of Biochemical Engineering, University College London, London, UK

Abstract

Three-dimensional (3D) cell cultures, such as spheroids, are essential for replicating *in vivo* tumor environments, offering a more accurate model for cancer research and drug testing. Spheroids form through the self-aggregation of cells under specific conditions, enabling the study of cellular behavior, including invasiveness. In this study, we investigated the correlation between spheroid formation ability and the reported invasiveness of four widely used human cancer cell lines — Human Embryonic Kidney 293 (HEK-293), Human Colorectal Adenocarcinoma (HT-29), Human Breast Cancer (MDA-MB-231), and Human Cervical Cancer (HeLa) — using a commercial round bottom 96-well microplate and AggreWell™ microwells with varying cell seeding concentrations. Cells were cultured in highly viscous media and seeded at varying densities (1,000, 2,000, and 3,000 cells per well) to assess the effect of cell number on spheroid size over time. Microscopic analysis revealed distinct differences among the cell lines; HEK-293 and HT-29 cells formed compact, well-defined spheroids, with larger spheroids observed at higher seeding densities. In contrast, the more aggressive and invasive MDA-MB-231 and HeLa cells failed to form spheroids under these conditions. These findings demonstrate the intricate relationship between cancer cell aggressiveness, seeding density, and spheroid formation ability, which are critical factors in optimizing 3D culture-based drug development and cancer research

Keywords: 3D cell culture, Spheroid formation, Cancer cell lines, Tumor invasiveness, Seeding density, Drug testing models

I. INTRODUCTION

The development of novel therapeutics and advanced drug delivery systems for genetic disorders, particularly cancer, has become a major area of research focus. Cancer alone accounted for nearly 10 million fatalities globally in 2020 [1]. Despite significant efforts, the rate of successful drug approvals remains relatively low, largely due to the lack of robust biological models that can effectively replicate the complexity of *in vivo* environments [2]. To address this challenge, there is a critical need to enhance preclinical testing platforms. By employing more physiologically relevant and efficient systems, researchers can improve the accuracy of drug evaluations, thereby increasing the likelihood of successful clinical translation and regulatory approval. For many years, drug screening has primarily relied on traditional 2D cell cultures, where cells grow in a single layer on flat surfaces [3]. This method is cost-efficient and well-studied [4]. However, 2D cultures have significant limitations. Cells grown in this environment lack the complex interactions seen in living tissues, as they cannot fully connect or communicate with one another. Additionally, during drug testing, the uniform exposure of cells to drugs does not reflect the natural conditions of tissues. This creates an oversimplified model that fails to capture the intricate dynamics of cell behavior and communication [5]. To address these shortcomings, there is a growing need for more advanced systems that better replicate the conditions of living organisms. As a result, 3D cell cultures have gained prominence as a superior alternative, and offer a more accurate representation of drug absorption and metabolic processes, closely mirroring *in vivo* conditions.

Three-dimensional (3D) cell culture systems play a pivotal role in tissue engineering and have been used as excellent platforms to create tissue-like structures that closely resemble *in vivo* conditions. These systems are broadly categorized into two methodologies: the "top-down" and "bottom-up" approaches [6]. In the top-down approach, cells are seeded onto 3D porous scaffolds that serve as temporary support structures [7]. As cells proliferate, the scaffold gradually degrades, allowing the formation of tissue-like constructs. However, this method often faces limitations, such as uneven cell distribution and challenges in accurately replicating the complexity of natural tissues [8]. To overcome these drawbacks, the bottom-up approach has gained prominence since the early 2000s [7]. This method relies on the creation of spheroids, which act as fundamental building blocks for constructing artificial tissues and organs [9]. Spheroid formation is driven by intricate cell-to-cell communication mechanisms, including the activation of integrins and the expression of cadherins, which are transmembrane proteins essential for cell adhesion [10]. These molecular interactions result in realistic cellular behavior and enable cells to respond more accurately to external stimuli. As a result, spheroids have emerged as highly promising tools in biomedical research, offering enhanced physiological relevance for applications such as drug testing and disease modelling.

Spheroids are widely utilized in various fields of biomedical research, including regenerative medicine for constructing 3D tissue models, drug metabolism studies to understand drug mechanisms and physiological responses, and, most notably, in cancer research as dynamic micro-tumor models to assess the efficacy of novel therapeutic agents [10]. To accurately evaluate the potential of cancer drug formulations, it is crucial to develop spheroid models with optimized properties. Under ideal conditions, cells can autonomously organize into spheroids through a process known as self-assembly, which occurs *in vitro* without external manipulation [11]. To facilitate this, commercially available platforms have been designed to promote self-organization by minimizing cell adhesion to surfaces, thereby encouraging cell-cell interactions [12]. Advances in science and technology have led to the development of diverse spheroid formation platforms, including magnetic levitation [13], hanging-drop methods [14], and suspension cultures [15]. Among these, commercial tools such as round-bottom microplates or AggreWell™800 microwells have gained significant attention due to their ability to enhance spheroid formation. The round-bottom design is particularly advantageous as it promotes the natural aggregation of cells into a single focal point, facilitating the formation of uniform and well-defined spheroids. Additionally, these microplates enable the simultaneous generation of a large number of spheroids in a single experiment, significantly

enriching statistical data and improving the reliability of experimental outcomes.

In this study, the spheroid-forming capabilities of four distinct cell lines—HEK-293, HT-29, MDA-MB-231, and HeLa—each exhibiting varying levels of invasiveness, were compared. The findings revealed significant differences in their ability to form spheroids under identical conditions. While HEK-293 and HT-29 cells consistently formed compact, well-defined spheroids, particularly at higher seeding densities, the more invasive MDA-MB-231 and HeLa cells failed to aggregate into spheroids using commercial spheroid-forming platforms. It should be noted that HeLa cells have been shown to form spheroids under different culture conditions and techniques in previous studies [16]. However, spheroid formation capacity may vary depending on factors such as culture medium composition, use of extracellular matrix components, and even the specific HeLa subline used, which can be genetically modified or adapted for 3D culture applications. Our results show the critical role of cellular invasiveness and seeding density in spheroid formation, which potentially suggests that highly aggressive cancer cells may resist self-assembly due to their migratory and invasive nature and may require more specific culture conditions. Unlike previous studies that have focused solely on spheroid formation efficiency, our work highlights the influence of both seeding density and platform type on the behavior of aggressive cancer cell lines in viscous culture media. This comparison reveals overlooked limitations of widely used cell lines in low-cost 3D culture setups. While the spheroid formation ability of cancer cells has been investigated in previous studies, direct comparisons correlating this ability with reported invasive and aggressive characteristics of cancer cell lines remain limited. In this context, we aimed to provide a quick and accessible reference using standardized 3D culture techniques to explore how reported invasiveness might influence spheroid formation behavior. In this context, our study aimed to provide a quick and accessible reference using standardized 3D culture techniques. We believe such a comparative report is valuable for understanding how these biological features can influence spheroid formation, even under optimized and widely used culture conditions. We believe these insights provide valuable understanding into why certain cell types are more challenging to model in 3D cultures.

II. MATERIAL AND METHODS

2.1. Material

The HEK-293 (human embryonic kidney cells), HeLa (human cervical cancer cells), HT-29 (human colon adenocarcinoma cells), and GFP-labeled MDAMB-231 (human breast cancer cells) were generously provided by the Biochemical Engineering Department at University College London (UCL), located in London,

United Kingdom. For cell detachment during subculturing, a trypsin enzyme solution derived from bovine pancreas was utilized, sourced from Sigma-Aldrich (St. Louis, MO, USA). The culture medium used for the experiments was FluoroBrite™ DMEM, a specialized formulation from Gibco designed to minimize background fluorescence by 90% compared to standard phenol red-free media. This medium was supplemented with GlutaMAX™, obtained from Gibco, and fetal bovine serum (FBS), procured from Thermo Fisher Scientific, to support cell growth and viability. Phosphate-buffered saline (PBS), also purchased from Gibco, was used for washing steps during cell culture procedures. To assess cell viability and transfection efficiency, staining solutions such as propidium iodide and Hoechst 33342 were employed, both sourced from Chemometec (Denmark). These dyes were used to distinguish between live and dead cells. Additionally, the NC-Slide A8™, purchased from Chemometec, was utilized for counting the cells and analyzing their viability.

2.2. Animal cell culture

HEK-293, HT-29, MDA-MB-231, and HeLa cell lines were cultured in FluoroBrite™ Dulbecco's Modified Eagle Medium (DMEM) supplemented with 10% fetal bovine serum (FBS) and 4 mM GlutaMAX™ to support optimal cell growth and viability. The cells were routinely passaged every 2 to 3 days to maintain them in an exponential growth phase. For subculturing, the cells were grown in T25 cell culture flasks featuring the Thermo Scientific™ Nunclon™ Delta surface, which is specifically designed to enhance cell adhesion and proliferation. The flasks were incubated in a humidified environment at 37°C with 5% CO₂ to mimic physiological conditions and ensure consistent cell growth. During passaging, cells were detached using a standard trypsin-EDTA solution, counted, and reseeded at appropriate densities to maintain healthy and confluent cultures.

2.3. Spheroid Formation in Commercial Round Bottom Microplate

The aforementioned cell lines were tested for their ability to form spheroids in commercial 96-well clear round bottom TC-treated microplate (Corning, USA). Once 90% of cell confluency was achieved in T25 flask, the cells were dissociated from the surface of culture flask and counted using NucleoCounter® NC-3000™ (Chemometec) using Via1-Cassette™ that contains two immobilized fluorophores, acridine orange (AO) and DAPI. For spheroid formation in round bottom microplate, highly-viscous culture media solution was prepared using 10% METHOCEL® cellulose ethers with 90% of FluoroBrite DMEM containing 10% FBS and Glutamax. After pouring 100 µL of methocel-containing culture media, the cell concentrations of 1000, 2000, and 3000 were seeded into each well of microplate.

2.4. Spheroid Formation in Commercial Round Bottom Microplate

For spheroid formation in AggreWell™800 plate, microwells were first pre-treated with 500 µL of AggreWell™800 Rinsing Solution and centrifuged at 2000 x g for 5 min using a rotor fitted with plate holders. Once the surface treated with rinsing solution, it was removed from microwells and was aspirated and microwells were rinsed with 2 mL of warm basal medium. Afterward, 2 mL of warm FluoroBrite DMEM containing cell suspension (3,000 cells per microwell) was added into wells and the plate was centrifuged at 100 x g for 3 min to capture HeLa cells in the microwells. After two days of incubation, the microplates were analyzed under the fluorescent microscope to evaluate the spheroid formation of each cell.

2.5. Morphological Analysis

The formation of spheroids was monitored and visualized using the EVOS™ Digital Color Fluorescence Microscope (Invitrogen). Images were captured daily under bright field illumination to assess the morphological characteristics of the spheroids. The morphological characteristics of spheroids, including their diameter and circularity, were quantified by processing bright-field images using ImageJ software. For circularity measurements, the corresponding images were first imported into ImageJ. Prior to analysis, each image was converted to a binary format to distinguish the spheroid structures from the background. Circularity analysis was performed using the built-in plugin developed by Wayne Rasband (wsr@nih.gov). The measurement settings were configured by selecting the "Circularity" parameter within the "Set Measurements" option under the "Analyze" menu. Individual spheroids were manually outlined using the "Freehand Selections" tool to ensure accurate boundary detection. Following this, the "Measure" function was applied to calculate the circularity of each spheroid based on the formula: $\text{circularity} = 4\pi(\text{area}/\text{perimeter}^2)$. This procedure was repeated for all spheroids present in the image set. The resulting circularity values were collected and subsequently used for further quantitative analysis and interpretation.

2.6. Morphological Analysis

The differences in spheroid formation among the two cell lines during 4 days, as well as the variations observed between different seeding concentrations (1,000, 2,000, and 3,000 cells per well), were statistically analyzed. Quantitative experiments were conducted at least in triplicates to ensure reproducibility and reliability of the data. Statistical analysis was performed using GraphPad Prism software, and significance was determined using appropriate statistical tests. For this, ordinary one-way ANOVA was employed and $p < 0.05$ was considered

significantly different. Results are presented as mean \pm standard deviation.

III. RESULTS AND DISCUSSION

3.1. Spheroid formation ability in round bottom microplate

In our study, different cancer cell lines (HEK-293, HT-29, MDA-MB-231, and HeLa) were tested in Corning® 96-well clear round bottom TC-treated microplate and AggreWell™800 as a commercial kit to evaluate their ability to form spheroids. Among the four cell lines, only HEK-293 is not a cancer-derived line; however, due to its immortalized nature, well-characterized growth properties, and widespread use as a control model in cancer research, we included HEK-293 cells in this study to provide a relevant reference point for comparing spheroid formation with cancerous cell lines [17]. Culture media was prepared using 10% METHOCEL® cellulose ethers for spheroid formation in microplate. According to the images acquired under the microscope, it was confirmed that both HeLa and MDAMB-231 cell lines couldn't form spheroids (Figure 2). In hypothesis, the cancer cells (e.g. HeLa and MDA-MB-231) with significantly more aggressive and invasive characteristics may possess certain difficulties to form spheroids as they want to expand rapidly instead of pattern-driven uniform self-assembly. On the other hand, HT-29 and HEK-293 cell lines are considerably less aggressive and formed spheroids with exceptional circularity and rigidity (Figure 2). Another crucial parameter that may perturb the formation of spheroid is the effect of culture medium. METHOCEL® is a water-soluble methylcellulose and hydroxypropyl methylcellulose polymers and was used to increase the viscosity of tissue-culture fluids for spheroid formation. The advantage of this gel is that the spheroids can be easily separated by cooling the culture medium in a refrigerator for a short period of time, during which the gel liquefies, enabling it to be facilely removed by pipetting. Due to its highly viscous characteristics, it may restrict the movement of aggressive cell lines and consequently induce slight changes in their metabolic pathways that impede them to form spheroids.

As shown in Figure 1, spheroid size increased over time in all seeding density groups, indicating continuous cell proliferation and compact spheroid formation. Higher initial cell numbers resulted in larger spheroids at each time point, which shows the influence of seeding density on spheroid growth dynamics. Statistical analysis confirmed significant size differences between groups, except between spheroids formed from 2000 and 3000 cells on day 1, where no significant difference was observed.

These findings are in line with previous literature highlighting the aggressive and invasive characteristics of MDA-MB-231 and HeLa cells compared to less aggressive lines such as HEK-293 and HT-29. Our results further suggest that this aggressive phenotype may act as a limiting factor for spheroid formation in simple low-cost 3D culture platforms. Our observations align with previous studies indicating that MDA-MB-231 cells require extracellular matrix components, such as collagen I, to effectively form spheroids. Specifically, it has been demonstrated that in the absence of collagen I, MDA-MB-231 cells fail to form spheroids; however, supplementation with collagen I facilitates spheroid formation with defined boundaries. This suggested that the methylcellulose-based medium used in our study did not provide the necessary extracellular matrix support for spheroid formation in these aggressive cell lines. This addition clearly demonstrates the importance of selecting appropriate culture conditions tailored to the specific characteristics of each cell line, particularly when working with aggressive cancer cells like MDA-MB-231. It also highlights the necessity of incorporating suitable extracellular matrix components to facilitate spheroid formation in such contexts. It is important to note that the aggressiveness and invasiveness of such cell lines discussed here are based on their widely reported behavior in the literature [18–20]. Our study did not directly measure invasiveness but rather assessed the spheroid formation ability of these cell lines in relation to their known biological characteristics. Such a measurement can be performed by well reported 3D tumor spheroid invasion assays [21].

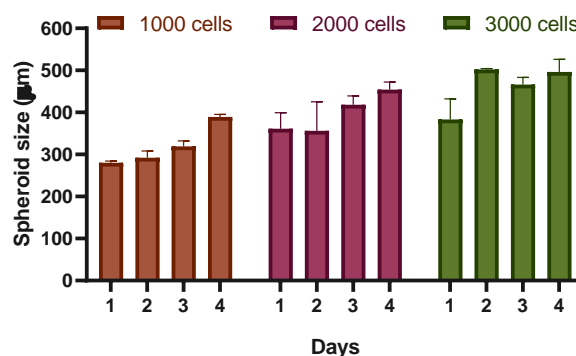


Figure 1. Growth profiles of spheroids formed with different initial cell numbers (1000, 2000, and 3000 cells per spheroid) over 4 days. Spheroid size was measured based on diameter using ImageJ analysis. Data are presented as mean \pm standard deviation ($n = 3$). According to one-way ANOVA, spheroid size significantly increased within each seeding density group over time (days 1 to 4). Additionally, spheroid sizes were significantly different between groups seeded with 1000, 2000, and 3000 cells at each respective day, except between 2000 cells (day 1) and 3000 cells (day 1), where no significant difference was observed.

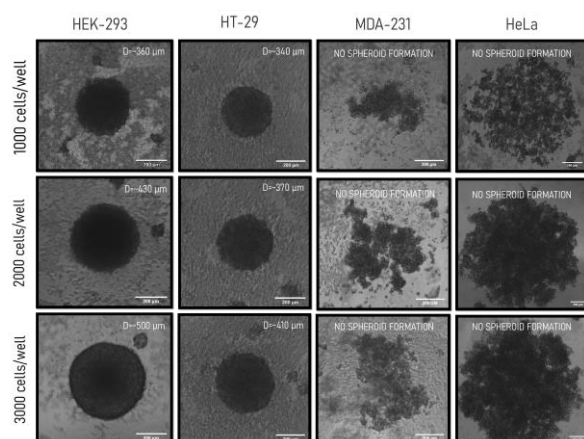


Figure 2. Bright-field images of cell lines tested for their ability of forming spheroids in Corning® 96-well clear round bottom TC-treated microplate. The images were taken on the 4th day after the first seeding ($t=1^{\text{st}}$ day). The scale bar represents 200 μm .

Cancer cell aggressiveness is a multifactorial and multidimensional aspect that cannot be solely described by a single parameter such as proliferation rate. While doubling time provides useful information regarding the proliferative capacity of cells *in vitro*, aggressiveness also encompasses characteristics such as invasiveness, migratory behavior, epithelial-to-mesenchymal transition, and resistance to cell death. In particular, highly invasive cancer cells often exhibit slower proliferation rates, as their phenotypic shift towards mesenchymal traits prioritizes migration over rapid cell division. This is commonly observed in mesenchymal-like breast cancer cells such as MDA-MB-231, which display high motility and reduced spheroid formation capacity despite a moderate doubling time. Conversely, epithelial-like cancer cells, such as HT-29, are characterized by rapid proliferation but lower invasive potential, facilitating compact spheroid formation in 3D cultures. Interestingly, HeLa cells, although fast-growing, often form less compact spheroids, possibly due to their partial epithelial phenotype and high proliferation-driven organization rather than cell-cell adhesion strength. Therefore, the ability of cancer cells to form spheroids is influenced by a complex interplay between proliferation, adhesion, and invasiveness, reflecting their diverse tumorigenic behaviors. The detailed characteristics of the cell lines used in this study, including cancer type, tumor classification, doubling time, and general aggressiveness profile, together with their corresponding Cellosaurus IDs, are summarized in Table 1. Cellosaurus is a widely used and curated cell line knowledge resource that provides standardized information about cell line origin, properties, and experimental use [22].

Table 1. Summary of cancer type, tumor classification, doubling time, and general aggressiveness profile of the selected cell lines used in this study. The Cellosaurus IDs of each cell line are also provided for reference. Doubling times were extracted from Cellosaurus, which cites different studies reported on the given cell line.

Cell Line	Cancer Type	Tumor Classification	Doubling Time	Invasiveness	General Aggressiveness Profile	Cellosaurus ID	Ref
MDA-MB-231	Breast adenocarcinoma	Triple-negative, invasive ductal carcinoma (mesenchymal-like)	~25-42 h	89% \pm 4% of cells invaded within the 48 h of culture	High invasiveness, high motility, poor spheroid formation	CVCL_0062	[23]
HeLa	Cervical carcinoma	HPV18-positive epithelial-like carcinoma	~31-48 h	Reported as aggressive	Fast proliferation, moderate invasiveness, variable spheroid formation	CVCL_0030	[24]
HT-29	Colorectal adenocarcinoma	Moderately differentiated colon cancer (epithelial-like)	~19.5-40 h	1.8% (range: 0-2.9%) of seeded cells invaded within 40 hours	Fast proliferation, low invasiveness, compact spheroid formation	CVCL_0320	[25]
HEK293	Embryonic kidney	Immortalized human embryonic kidney cells	~24-30 h	No aggressiveness	Non-tumorigenic, non-invasive, no spheroid formation tendency	CVCL_0045	[26]

3.2. Spheroid formation ability in AggreWell™800

Bearing in mind this hypothesis, we tested AggreWell™800 (STEMCELL Technologies), a platform specifically designed for 3D cell cultures, to evaluate the spheroid formation ability of HeLa cells, which failed to form spheroids in commercial round bottom microplates. Unlike the Corning 96-well clear round bottom TC-treated microplates, which require the use of METHOCEL® to increase medium viscosity and restrict cell movement, the AggreWell™800 system uses liquid culture media, facilitating enhanced cell aggregation. The geometry of AggreWell™800, featuring square-shaped microwells, ensures uniform cell distribution and guides cells toward the center, making it a more potent platform for 3D cell culture compared to traditional round bottom microplates (Figure 3).

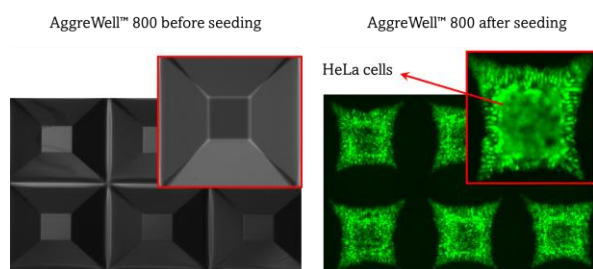


Figure 3. Microscopic images of AggreWell™800, a commercial platform designed specifically for 3D cell cultures. The image on the left shows empty AggreWells before cell seeding, while the image on the right illustrates AggreWells seeded with HeLa cells, demonstrating the initial distribution of cells within the wells.

To verify whether the inability to form spheroids was due to the platform or the intrinsic nature of HeLa cells, we conducted this experiment solely with HeLa cells. The cells were analyzed over an 8-day period (Figure 4), and at the end of the incubation, an attempt was made to retrieve the spheroids using a pipette specifically designed for spheroid handling. However, the retrieved structures were neither rigid nor round, with cells not efficiently attached to one another (Figure 5). This observation led to the conclusion that the inability to form spheroids was inherent to the nature of HeLa cells, as even the optimized AggreWell™800 platform could not facilitate proper spheroid formation.

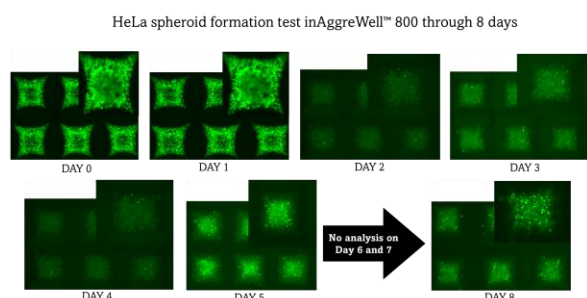


Figure 4. Fluorescent microscopic images showing HeLa cells cultured in AggreWell™800 over 8 days. The progression of cell aggregation is observed across the time points, with the initial clustering evident on Day 1. However, the cells failed to form rigid and cohesive spheroids, with the structures remaining loose and irregular throughout the culture period. No analysis was performed on Days 6 and 7. The inset images highlight the central aggregation of cells within the AggreWell microwells at specific time points.

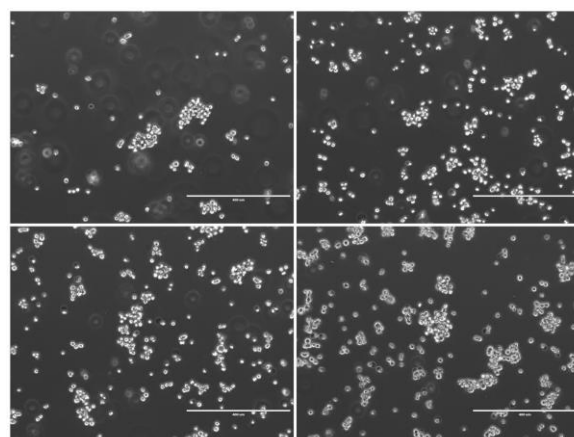


Figure 5. Microscopic image of HeLa cells after removal from AggreWell™800 and subsequent seeding onto a round cell culture flask. The cells are observed in aggregated or single-cell forms, with no visible spheroid structures. The scale bar represents 400 μm in all pictures.

3.3. Viability of Cells Forming Spheroids

To investigate whether the inability of HeLa cells to form spheroids in AggreWell™800 was due to a lack of cellular health, we analyzed the viability of HeLa cells cultured in the platform. After removing the cells from the wells, their viability was assessed using Via1-Cassette™ in the NucleoCounter® NC-3000™. The NucleoCounter® NC-3000™ utilizes Via1-Cassette™, a specialized consumable containing two immobilized fluorophores, acridine orange (AO) and DAPI. Acridine orange is a cell-permeable dye that intercalates with DNA in both live and dead cells, emitting a green fluorescence. DAPI, on the other hand, is impermeable to live cells and specifically stains the nuclei of dead cells, emitting a blue fluorescence. According to our measurements, cell viability of HeLa cells was over 90% after culturing in AggreWell™800 for 7 days, showing the cells were healthy and couldn't form spheroids due to their nature.

IV. CONCLUSION

3D spheroid models are invaluable tools in cancer research and offer more physiologically relevant platforms compared to traditional 2D cultures for studying tumour biology, drug response, and cellular behaviour. This study highlighted the variability in spheroid-forming ability among four distinct cell lines—HEK-293, HT-29, MDA-MB-231, and HeLa—using commercial platforms such as round bottom microplates and AggreWell™800. While HEK-293 and HT-29 cells formed compact, well-defined spheroids, the aggressive and invasive MDA-MB-231 and HeLa cells failed to form cohesive spheroids, even under optimized conditions. These findings show the critical role of cell line characteristics, such as invasiveness and aggregation potential, in determining their suitability for 3D culture systems. Furthermore, the viability analysis confirmed that the inability of HeLa cells to form spheroids was not due to poor

cellular health but rather an intrinsic property of the cell line. This study draws attention to practical limitations in spheroid formation for commonly used aggressive cancer cell lines. Our observations suggest that even with optimized platforms, certain cell lines may not be suitable for standard 3D drug testing models. While the use of methylcellulose-based media and standard round-bottom plates is well established, our study highlights that cellular aggressiveness — particularly invasiveness — may considerably limit spheroid formation even under optimized conditions. While we did not experimentally evaluate invasiveness parameters such as migration or invasion assays, our study provides insight into how reported aggressive characteristics of certain cell lines might influence their ability to form spheroids under standardized 3D culture conditions. We hope this study provides a practical reference for researchers when selecting appropriate 3D culture models, especially for aggressive cancer cell lines commonly used in drug testing. Understanding these differences is essential for selecting appropriate models in 3D culture-based cancer research and for improving the development of therapeutic strategies targeting tumor heterogeneity.

ACKNOWLEDGEMENT

Ismail Eş acknowledges the financial support of Sao Paulo Research Foundation (FAPESP), Brazil (Grant# 2015/14468-0 and 2018/23895-7)

REFERENCES

- [1] Ferlay, J., Colombet, M., Soerjomataram, I., Parkin, D.M., Piñeros, M., Znaor, A., & Bray, F. (2021). Cancer Statistics for the Year 2020: An Overview. *International Journal of Cancer*, 149, 778-789.
- [2] DiMasi, J.A., Reichert, J.M., Feldman, L., & Malins, A. (2013). Clinical Approval Success Rates for Investigational Cancer Drugs. *Clinical Pharmacology & Therapeutics*, 94, 329-335.
- [3] Wei, F., Wang, S., & Gou, X. (2021). A Review for Cell-based Screening Methods in Drug Discovery. *Biophysics Reports*, 7, 504.
- [4] Kapalczyńska, M., Kolenda, T., Przybyła, W., Zajączkowska, M., Teresiak, A., Filas, V., Ibbs, M., Bliźniak, R., Łuczewski, Ł., & Lamperska, K. (2018). 2D and 3D Cell Cultures - A Comparison of Different Types of Cancer Cell Cultures. *Archives of Medical Science*, 14, 910-919.
- [5] Fang, Y., & Eglen, R.M. (2017). Three-dimensional Cell Cultures in Drug Discovery and Development. *SLAS Discovery: Advancing Life Sciences R&D*, 22, 456-472.
- [6] Dyson, P.J. (2019). The Rise of 3D Cellular Spheroids: Efficient Culture via Upward Growth from a Superamphiphobic Surface. *National Science Review*, 6, 1068-1069.
- [7] Wang, X., Wang, Z., Zhai, W., Wang, F., Ge, Z., Yu, H., & Yang, W. (2021). Engineering Biological Tissues from the Bottom-up: Recent Advances and Future Prospects. *Micromachines*, 13, 75.
- [8] Antoni, D., Burckel, H., Josset, E., & Noel, G. (2015). Three-dimensional Cell Culture: A Breakthrough in Vivo. *International Journal of Molecular Sciences*, 16, 5517-5527.
- [9] Kronemberger, G.S., Matsui, R.A.M., de Castro, G.A.S., Granjeiro, J.M., & Baptista, L.S. (2020). Cartilage and Bone Tissue Engineering Using Adipose Stromal/Stem Cells Spheroids as Building Blocks. *World Journal of Stem Cells*, 12, 110.
- [10] Ryu, N.E., Lee, S.H., & Park, H. (2019). Spheroid Culture System Methods and Applications for Mesenchymal Stem Cells. *Cells*, 8, 1620.
- [11] Roy, S.M., Garg, V., Barman, S., Ghosh, C., Maity, A.R., & Ghosh, S.K. (2021). Kinetics of Nanomedicine in Tumor Spheroid as an In Vitro Model System for Efficient Tumor-targeted Drug Delivery with Insights from Mathematical Models. *Frontiers in Bioengineering and Biotechnology*, 9, 785937.
- [12] Morán, M.C., Cirisano, F., & Ferrari, M. (2023). Spheroid Formation and Recovery Using Superhydrophobic Coating for Regenerative Purposes. *Pharmaceutics*, 15, 2226.
- [13] Gaitán-Salvatella, I., López-Villegas, E.O., González-Alva, P., Susate-Olmos, F., & Álvarez-Pérez, M.A. (2021). Case Report: Formation of 3D Osteoblast Spheroid Under Magnetic Levitation for Bone Tissue Engineering. *Frontiers in Molecular Biosciences*, 8, 672518.
- [14] Rasouli, M., Safari, F., Kanani, M.H., & Ahvati, H. (2024). Principles of Hanging Drop Method (Spheroid Formation) in Cell Culture. Springer.
- [15] Anil-Inevi, M., Yaman, S., Yildiz, A.A., Mese, G., Yalcin-Ozuysal, O., Tekin, H.C., & Ozcivici, E. (2018). Biofabrication of In Situ Self Assembled 3D Cell Cultures in a Weightlessness Environment Generated Using Magnetic Levitation. *Scientific Reports*, 8, 7239.
- [16] Minamikawa-Tachino, R., Ogura, K., Ito, A., & Nagayama, K. (2020). Time-lapse Imaging of HeLa Spheroids in Soft Agar Culture Provides Virtual Inner Proliferative Activity. *PLoS One*, 15, e0231774.
- [17] Stepanenko, A.A., & Dmitrenko, V.V. (2015). HEK293 in Cell Biology and Cancer Research: Phenotype, Karyotype, Tumorigenicity, and Stress-induced Genome-phenotype Evolution. *Gene*, 569, 182-190.

- [18] Gest, C., Joimel, U., Huang, L., Pritchard, L.L., Petit, A., Dulong, C., Buquet, C., Hu, C.Q., Mirshahi, P., & Laurent, M. (2013). Rac3 Induces a Molecular Pathway Triggering Breast Cancer Cell Aggressiveness: Differences in MDA-MB-231 and MCF-7 Breast Cancer Cell Lines. *BMC Cancer*, 13, 1-14.
- [19] Sukjoi, W., Young, C., Acland, M., Siritutsoontorn, S., Roytrakul, S., Klingler-Hoffmann, M., Hoffmann, P., & Jitrapakdee, S. (2024). Proteomic Analysis of Holocarboxylase Synthetase Deficient-MDA-MB-231 Breast Cancer Cells Revealed the Biochemical Changes Associated with Cell Death, Impaired Growth Signaling, and Metabolism. *Frontiers in Molecular Biosciences*, 10, 1250423.
- [20] Zhong, Z., Pannu, V., Rosenow, M., Stark, A., & Spetzler, D. (2018). KIAA0100 Modulates Cancer Cell Aggression Behavior of MDA-MB-231 Through Microtubule and Heat Shock Proteins. *Cancers*, 10, 180.
- [21] Vinci, M., Box, C., & Eccles, S.A. (2015). Three-dimensional (3D) Tumor Spheroid Invasion Assay. *Journal of Visualized Experiments: JoVE*, 52686.
- [22] Bairoch, A. (2018). The Cellosaurus, a Cell-line Knowledge Resource. *Journal of Biomolecular Techniques: JBT*, 29, 25.
- [23] Ellis, K., & Wood, R. (2023). The Comparative Invasiveness of Endometriotic Cell Lines to Breast and Endometrial Cancer Cell Lines. *Biomolecules*, 13, 1003.
- [24] Lucey, B.P., Nelson-Rees, W.A., & Hutchins, G.M. (2009). Henrietta Lacks, HeLa Cells, and Cell Culture Contamination. *Archives of Pathology & Laboratory Medicine*, 133, 1463-1467.
- [25] De Both, N.J., Vermey, M., Dinjens, W.N., & Bosman, F.T. (1999). A Comparative Evaluation of Various Invasion Assays Testing Colon Carcinoma Cell Lines. *British Journal of Cancer*, 81, 934-941.
- [26] Alberti, L., Losi, L., Leyvraz, S., & Benhattar, J. (2015). Different Effects of BORIS/CTCF on Stemness Gene Expression, Sphere Formation and Cell Survival in Epithelial Cancer Stem Cells. *PLoS One*, 10, e0132977.